Multilayered bioactive composite coatings with drug delivery capability by electrophoretic deposition combined with layer-by-layer deposition

Q. Chen[1], Y. Liu[2], Q.Q. Yao[3], S.S. Yu[3], K. Zheng[1], M. Pischetsrieder[2], and A.R. Boccaccini[1]*

[1] Institute of Biomaterials, Department of Materials Science and Engineering, University of Erlangen-Nuremberg, Erlangen, 91058 Germany
[2] Department of Chemistry and Pharmacy, Food Chemistry, University of Erlangen-Nuremberg, Erlangen, 91052 Germany
[3] Institute of Advanced Materials for Nano-Bio Applications, School of Ophthalmology & Optometry, Wenzhou Medical University, Zhejiang, 325027 China

A combination of electrophoretic deposition and layer-by-layer deposition was applied to fabricate multilayered bioactive coatings consisting of hydroxyapatite and biodegradable polymers including alginate, chitosan and polyvinyl alcohol. The bottom layer, namely hydroxyapatite/alginate composite, was deposited onto stainless steel substrates by one-step electrophoretic deposition. The second layer made of alginate and polyvinyl alcohol was also deposited by electrophoretic deposition, and then layer-by-layer was introduced for the deposition of chitosan and alginate layers. A range of characterization methods including scanning electron microscopy, Fourier transform infrared spectroscopy and laser profilometer were used to evaluate the compositional and microstructural properties of the deposited multilayer coatings. The coatings showed a stable degradation rate, and superior bioactivity due to the presence of hydroxyapatite in the bottom layer. Furthermore, the burst release of lysozyme, which was selected as a model actibacterial agent in this study, was significantly suppressed and a sustained release up to 14 days was obtained. Cell viability and antibacterial tests of lysozyme-loaded multilayer coatings were carried out to confirm the suitability of the proposed coating system for multifunctional modification of opthopaedic implants and to validate the coating techniques involved.

Keywords: electrophoretic deposition, multilayer, hydroxyapatite, lysozyme, polyelectrolyte, drug delivery

1. Introduction

Metallic implants made of bioinert materials including stainless steel and titanium alloys tend to possess a weak connection with the surrounding tissue, which impairs the complete fixation of the device and may lead to implant failure. Consequently, in the field of orthopaedic implants, bioactive coatings consisting of bioceramics, biodegradable polymers and their combinations, are being intensively investigated in order to improve the implant–tissue bonding as well as to incorporate biological entities for accelerated bone regeneration [1–3]. On the other hand, infection is still one of the most extended complications related to orthopedic surgery [4]. This may affect the healing process and lead to lengthy medication treatment, or even complete failure of the implant which is a serious problem and has clinical and economic consequences [5]. The most common methods used to treat implant related infections are the pre- and postoperative medication of oral or intravenous injected antibiotics [6]. Recently, incorporation of biomaterial coatings containing bactericidal molecules is gaining increasing attention [2, 7]. In comparison with traditional anti-infection methods, coated implants could serve as a local drug delivery system to treat infections with high local dosage, long-term controlled release and lower risk of systemic toxicity [8].

Electrophoretic deposition (EPD) is a cost-effective and versatile coating technique being increasingly used to manipulate charged particles and molecules in suspension to form a variety of bulk materials and coatings [9, 10], especially its application in the field of biomaterial coatings has been widely considered in the last few years [11, 12]. Several bioceramic–biopolymer composite coatings, such as the combination of bioceramics (hydroxyapatite (HA) or bioactive glass) with biopolymers, have been successfully fabricated by electrophoretic deposition, and desirable bioactivity, measured by the rapid hydroxyapatite formation

* *Corresponding author*
Prof. Dr. Aldo R. Boccaccini, aldo.boccaccini@ww.uni-erlangen.de

on the surface upon immersion in simulated body fluid, was achieved [13, 14]. Hydroxyapatite is an important bioactive additive as its chemical composition is similar to the composition of the mineral phase of bone [15, 16]. Commonly used polymers for biomedical applications include alginate, chitosan, polyvinyl alcohol and a variety of natural and synthetic polymers which are biocompatible, biodegradable, low-toxic and cost-effective [17, 18]. Since electrophoretic deposition is a room-temperature coating process, it is interesting to consider the incorporation of antibacterial agents which can be directly added into the EPD suspension and co-deposited into the coating structure [7, 19]. Even if antibacterial agents including antibiotic drugs can be loaded simply within a carrier matrix by either physical embedding or covalent linking, the controlled release of antibiotics under physiological conditions with tunable dosage remains a challenge [20, 21]. For example, swelling or dissociation of the coating structure at the early stage after implantation can severely induce so-called "burst release" of the antibiotic, negating the desired sustained and controlled drug release. Indeed it is reported that the duration of drug release for the treatment of prosthetic-joint infection should be at least a few weeks [22].

Antibacterial coating systems fabricated by layer-by-layer (LbL) deposition are gaining increasing attention due to their simplicity, cost-effectiveness, reproducibility, and high versatility to tailor compositions, structures, properties, and functions in the nanoscale [23]. Layer-by-layer deposition is a coating technique that possesses unique characteristics compared to electrophoretic deposition. For example, the water electrolysis which usually happens during the electrophoretic deposition process does not exist with layer-by-layer deposition and in this case, the compact structure of the deposited coating could be maintained after repeated dipping cycles. However, layer-by-layer deposition is not as effective as electrophoretic deposition in controlling the arrangement and deposition of particles and molecules which is a direct effect of the electric field involved in electrophoretic deposition. In this study, a combination of electrophoretic deposition and layer-by-layer deposition is considered, exploiting the advantages of both coating methods (fast processing and strong manipulation of micron-sized particles by electrophoretic deposition and bubble-free and no limitation of deposited layers in layer-by-layer deposition), for the fabrication of multilayered bioactive coating with drug delivery capability. The bioceramic component (hydroxyapatite particles in the present case) embedded in the bottom layer is considered to support the bioactive character of the coating for a better bone-to-implant interaction, and the antibacterial agent incorporated in the subsequent layers should be released simultaneously taking into account postoperative inflammations associated with bacterial infection during the early stage after implantation. As a model for a water-soluble biomolecule, lysozyme, was introduced in this study to evaluate the drug release profile from the designed coating structure. In addition to presenting the basic characterization of the compositional and microstructural properties of the deposited coatings, the drug release profile as well as relevant biological tests of the lysozyme-loaded multilayer coatings, including cell viability and quantitative antibacterial tests, were carried out to evaluate the feasibility of the developed coating technique for fabrication of multifunctional bioactive coatings.

2. Experimental

2.1. Materials

Solid sodium alginate, chitosan (degree of deacetylation 75–85 %), acetic acid (purity ≥99.7 %), sodium acetate powder, phosphate buffered saline (PBS) tablets and chicken egg white lysozyme powders (14.307 kDa, ≥40000 units/mg protein) were obtained from Sigma-Aldrich (Steinheim, Germany). Commercial nano-hydroxyapatite powder was purchased from Merck (Belgium). The polyvinyl alcohol powder (fully hydrolyzed ~98 %; molecular weight ~30000) was acquired from Merck KGaA (Darmstadt, Germany).

2.2. Suspensions

The proposed multilayer structure is schematically shown in Fig. 1. Hydroxyapatite particles were embedded in alginate matrix in the bottom layer by electrophoretic deposition. With the same principle, lysozyme molecules were loaded in both the bottom layer and the second layer. A mixture of water and ethanol with a total volume of 50 ml was used as solvent for all EPD suspensions.

The EPD suspension for the bottom layer consisted of the following ingredients and concentrations: 2 mg/ml alginate, 10 mg/ml hydroxyapatite and 2 mg/ml lysozyme. Firstly alginate and lysozyme powders were completely dissolved in deionized water with magnetic stirring followed by 4 min of ultrasonic bath treatment (Bandelin Sonorex). Then 40 vol % of ethanol was added dropwise with simultaneous magnetic stirring until the blend solution became stable and transparent. Finally hydroxyapatite particles were homogeneously dispersed in the solution by applying magnetic stirring for 7 min and subsequent 30 s of ultrasonic bath treatment.

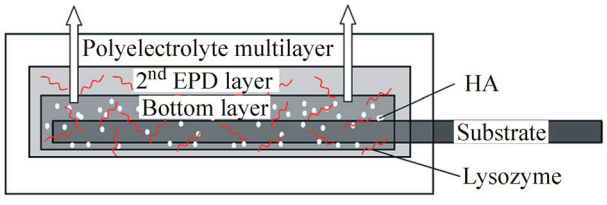

Fig. 1. Schematic diagram showing the arrangement of the multilayer structure of the deposited coatings.

The EPD solution of the second layer and the alginate/chitosan solutions of the polyelectrolyte multilayer were prepared as follows. The suspension for the second electrophoretic deposition layer consisted of 2 mg/ml alginate, 20 mg/ml polyvinyl alcohol and 2 mg/ml lysozyme. A basic solution of 50 mg/ml polyvinyl alcohol was prepared initially. Polyvinyl alcohol powder was dissolved in deionized water by heavily stirring for a few minutes at 80 °C until a clear solution was visible. For a 50 ml solution, 2 mg/ml alginate was mixed in a cold solution (60 vol %) of 10 ml de-ionized water mixed with 20 ml basic polyvinyl alcohol solution. 2 mg/ml lysozyme was added after the alginate was totally dissolved. Finally 20 ml (40 vol %) ethanol was added very slowly to a heavily stirred solution. 2 min of ultrasonic bath treatment was applied after each dissolution step to achieve a homogeneous dissolution of each component. Layer-by-layer deposition was used to fabricate polyelectrolyte multilayer structure after the second EPD process, and the corresponding chitosan (positively charged) and alginate (negatively charged) solutions were prepared according to the literature [24]. Briefly, an acetate buffer was prepared at pH 3 or 5 using appropriate volumes of 0.1 M acetic acid and 0.1 M sodium acetate, 5 mg/ml of alginate was prepared in the low pH buffer (pH = 3), and 1 mg/l of chitosan was prepared in the high pH buffer (pH = 5) with the help of magnetic stirring and ultrasonic bath.

2.3. Depositon procedure

For the EPD setup two parallel 316L stainless steel substrates ($30\times15\times0.2$ mm^3) separated a distance of 10 mm were used as electrodes and immersed into the prepared suspension. The plates were dipped 20 mm into the suspension yielding a deposition area of 20×15 mm^2. A trial-and-error approach was carried out to optimize electrophoretic deposition parameters for a robust and homogeneous two-layer electrophoretic deposition coating with the highest possible thickness. The optimized fabrication parameters are shown in Table 1. Anodic deposition of the bottom layers was obtained due to the negative charge of alginate in water [13]. For the fabrication of polyelectrolyte multilayer structure by layer-by-layer deposition, the obtained two-layer electrophoretic deposition coatings were dipped alternatively in chitosan and alginate solutions for 15 s, respectively. A total of 8 layers were obtained with an alginate-ending layer on the top. The coating was completely dried in-between all steps. It was also considered that the dipping depth for each electrophoretic deposition and layer-by-layer deposition step was always higher than that of the previous coating.

2.4. Characterization

2.4.1. Zeta potential measurement

The surface charge of hydroxyapatite particles was measured in terms of zeta potential by laser Doppler velocimetry (LDV) technique, using a Zetasizer nano ZS equipment (Malvern Instruments, UK). The laser Doppler velocimetry method measures the electrophoretic mobility of the particles and, after applying Henry's equation, transforms that value into zeta potential values. The solvent used for zeta potential measurement was a mixture of 60 vol % water and 40 vol % ethanol in accordance to the composition of the solvent used for electrophoretic deposition. The zeta potential of pure hydroxyapatite particles with a solid content of 0.1 mg/ml was measured as a reference. In order to detect the possible interactions between the particle and the polyelectrolyte chain, hydroxyapatite particles were added into a alginate solution with a solid content of 0.1 mg/ml, and the suspension was magnetically stirred overnight to ensure a complete interaction between each other. Then the particles were collected by centrifugation (Centrifuge 5416, Eppendorf, Germany) at 7830 rpm for 3 min, rinsed twice with deionized water and redispersed into water-ethanol solvent for zeta potential measurement.

2.4.2. Deposit yield measurement

The deposit mass after each coating process was measured with an analytical balance with an accuracy of 0.1mg and the deposit yield (deposit mass per unit area) was determined knowing the area of the deposit (20×15 mm^2).

2.4.3. Compositional and microstructural measurements

Fourier transform infrared spectroscopy (FTIR) was conducted (Nicolet 6700) in the wavenumber ranging from 400 to 4000 cm^{-1} by mixing the sample with KBr in the ratio 1:200 (w/w). To investigate the surface roughness a laser profilometer (UBM, ISC-2) was used. The scanning rate is 10 mm/min with a resolution of 1000 point/mm. Scanning electron microscopy (SEM, model Auriga, Zeiss) was applied to evaluate the morphology and microstructure of the obtained coatings after the different coating processes and treatment.

2.4.4. Bioactivity and degradation test

For the bioactivity assessment, the multilayer coatings were soaked in 50 ml of simulated body fluid (SBF) solu-

Table 1. Fabrication parameters of the multilayer coating.

Coating	Bottom layer		Second EPD layer		Polyelectrolyte layer	
Parameters	Deposition voltage, V	Deposition time, s	Deposition voltage, V	Deposition time, s	Chitosan dipping time, s	Alginate dipping time, s
	10	30	5	15	15	15

tion prepared according to the literature [25], and placed in an orbital shaker at 37 °C at an agitation rate of 90 rpm. The samples were incubated for up to 7 days and the simulated body fluid solution was replaced every two days. Three samples for each condition and time point were assessed. After incubation for fixed time points, the samples were removed, gently rinsed with deionized water for three times and dried at 37 °C in a desiccator for 24 h. SEM was applied to analyze the surface morphology of the coatings during the mineralization process in simulated body fluid.

Simulated body fluid was replaced with PBS solution for the degradation rate measurement. The weight of the coating after incubation in PBS for different periods was measured and the weight loss of the multilayer coating after incubation for different time points was recorded.

2.4.5. Drug release study

To analyze the lysozyme release profile, the lysozyme-containing multilayer coatings (in triplicate) were immersed in 2 ml of PBS and located in a 37 °C incubator for a sustained period of 2 weeks. After each pre-determined time point (0.5 h, 1 h, 2 h, 4 h, 8 h, 10 h, 1 d, 2 d, 4 d, 7 d, and 14 d), the whole solution was withdrawn and the released concentration of lysozyme was directly measured by UV-vis spectrophotometer (Specord 40, Analytic Jena, Germany) at the wavelength of 281 nm. Two millilitre of fresh PBS was refilled for a continuous release and detection. It should be noted that the concentration of a test lysozyme solution in a 37 °C incubator was not changed for up to 4 weeks, which confirms the stability of lysozyme structure during the measurement. The total release of lysozyme at each time point m_x could be calculated by accumulating the released lysozyme before that time. In order to calculate the percentage of lysozyme release ρ_x after each time point, the total amount of lysozyme in the coating should be determined. It is considered that the lysozyme-containing coatings with the same fabrication condition possess identical amount of lysozyme, then the total amount of lysozyme in the coating m_t was determined by scratching the whole area of a coating with the same condition into 2 ml of PBS and shaking it at 37 °C for three weeks. The percentage of cumulative release at each time point was obtained from m_t divided by m_x.

2.4.6. Cell viability assay

A cell viability study was conducted using a cell counting kit 8 (CCK-8, Beyondtime Bio-Tech, China). This kit allows the quantitative determination of the cell viability and cytotoxicity of the test sample. The sterilized samples (1×1 cm^2) were placed into a 24-well flat culture plate, and 1×10^4 cells/well was seeded into each well. The cells were cultured for 1, 2 and 4 days, respectively, then 20 μl CCK-8 reagent was added per well, and the cells were incubated for an additional 2 h. The results were expressed as percentage of the mean absorbance (optical density) of treated samples versus controls. The mean optical density of the blank control was set to represent 100 % viability.

2.4.7. Antibacterial test

The antibacterial activity of samples was evaluated using the 96-well plate assay as described by Pritchard et al [26]. *Escherichia coli* ATCC 25922 (*E. coli*) and *Bacillus subtilis* ATCC 6051, considered in this study as model bacteria from gram-negative and gram-positive bacteria families, respectively, were purchased from Leibniz Institute DSMZ-German Collection of Microorganisms and Cell Cultures (Braunschweig, Germany). According to the in structions of the manufacturer, both strains were inoculated into fresh nutrient broth (Roth, Karlsruhe, Germany) and incubated at 37 °C for 8 h simultaneously shaking to reach the logarithmic phase of growth at a density of $(1–5)\cdot10^7$ cfu/ml. Then, these bacterial suspensions were diluted to a density of $(1–5)\cdot10^5$ cfu/ml before use.

The minimal inhibitory concentration (MIC) of lysozyme was determined as its lowest concentration to effectively inhibit the bacterial growth. Lysozyme concentration was varied using two-fold serial dilutions ranging from 40 to 0.3125 μg/ml. Individual wells of a sterilized 96-well microtitre plate were inoculated with 50 μl of lysozyme solution and 50 μl of bacterial suspension. Control wells contained all the components except the test medium, which were replaced by 50 μl ampicillin (10 μg/ml, negative control) or 50 μl sterilized sodium phosphate buffer (10 mM, positive control). The experiment was conducted in triplicate and the optical density (OD, 600 nm) of samples incubated for 9 h at 37 °C was recorded spectrophotometrically by using a temperature-controlled automatic plate reader (Tecan, Männedorf, Switzerland). Percentage of bacterial growth was determined by Eq. (1):

$$\text{Bacterial growth (\%)} = \frac{(OD^{\text{sample}} - OD^{\text{negative control}})}{(OD^{\text{positive control}} - OD^{\text{negative control}})}\cdot 100\,\%. \quad (1)$$

To evaluate the antibacterial effect of the sustained release of lysozyme, three groups of lysozyme-containing coatings were immersed in 2 ml of PBS at 37 °C for 1, 3, 7 days, respectively. After the termination of each time point, the solution was completely renewed with identical amount of PBS and the samples were immersed continuously for another 12 h. The lysozyme concentration of the final solution was determined by UV-vis spectrophotometer as described previously. Then the antibacterial test was conducted following the procedure of the minimal inhibitory concentration measurement. Individual wells of a sterilized 96-well microlitre plate were inoculated with 50 μl of the specimen solution and 50 μl of bacterial suspension. Control wells contained all the components except the test medium, which was replaced by 50 μl ampicillin (10 μg/ml, negative control) or 50 μl sterilized sodium phosphate buffer (10 mM, positive control). The experiment was conducted in tripli-

cates and the optical density (600 nm) of samples incubated for 9 h at 37 °C (with shaking) was recorded spectrophotometrically by using a temperature-controlled automatic plate reader (Tecan, Männedorf, Switzerland). The percentage of bacterial growth was determined also according to Eq. (1).

3. Results and discussion

3.1. Deposition mechanism

According to the zeta potential measurement, as-received hydroxyapatite particles show positive surface charge (+12 ± 10 mV) in a water-ethanol solvent. However, the surface charge was reversed after thoroughly mixing with the alginate (–10 ± 10 mV), leading to the anodic deposition of hydroxyapatite as observed in the present experiments. The reversal of surface charge is likely due to the electrostatic adsorption of oppositely charged polymer chains on the particle surfaces. Therefore, it is suggested that, for example in the case of the EPD suspension used here, the negatively charged alginate migrates to the positive electrode dragging the wrapped hydroxyapatite particles in the same direction.

3.2. Deposit yield

Figure 2 shows the deposit yield of the deposited coating after each coating step. The first electrophoretic deposition step yields an average weight of 0.67 mg/cm^2 of alginate-hydroxyapatite composite. A significant increment (~1 mg/cm^2) after the second EPD process was obtained and with the increase of deposited layers by layer-by-layer technique, the deposit yield of the final multilayer coating reached a total deposit yield of 2.25 mg/cm^2. In an ideal condition of continuous electrophoretic deposition, the deposit yield could be accurately predicted according to Hamaker's law [27]. However it is difficult to establish a quantitative correlation to interpret the overall deposition profiles in the present study as different suspensions were applied and different coating techniques were involved at the same time. Considering the drug delivery application of the proposed coating system, it is of great importance to know the drug loading in the coating structure. The deposit yield at different coating steps can be then used to determine the total drug amount in the final multilayer coating.

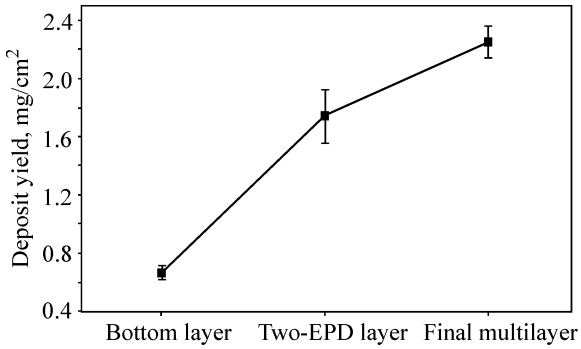

Fig. 2. Deposit yield after different coating stages.

3.3. Fourier transform infrared spectroscopy assessment

FTIR spectra of the multilayer coating before and after incubation in simulated body fluid for 2 and 7 days are shown in Fig. 3. The presence of alginate could be confirmed with the bands at 1620–1610 cm^{-1} for the asymmetric stretching of COO^- and 1430–1410 cm^{-1} for the symmetric stretching of COO^-. The presence of polyvinyl alcohol was confirmed by the OH stretching at 3350 cm^{-1} and the CH_2 stretching at 2947 cm^{-1} [14, 28, 29]. The vibrations associated with amide II (1629 cm^{-1}) and amide I (1552 cm^{-1}) groups became obvious in the spectrum of day 2 sample, as arrowed in the figure, which indicates the presence of chitosan in the coating [30]. It can be observed that all spectra present the vibration of double P-O band (561 cm^{-1} and 601 cm^{-1} as indicated in the figure) assigned to crystalline apatite [14]. The co-deposition of all coating components is confirmed according to FTIR measurement, however, FTIR results could not confirm the new hydroxyapatite formation as hydroxyapatite powder is one of the raw materials before simulated body fluid incubation.

3.4. SEM observations

Scanning electron microscopy (SEM) was carried to evaluate the microstructure of the deposited coatings and to observe in detail the connections between different layers. The surface image of a two-EPD layer structure is presented in Fig. 4a. Homogeneous and crack-free composite coatings were obtained with two separate EPD processes. Although the particles are completely wrapped by polymer components, the two-EPD layer coating presents a rough surface due to the presence of hydroxyapatite clusters, which is probably the reason for the high deposit yield. However, the surface of the final multilayer coating in Fig. 4b is quite smooth after the layer-by-layer deposition. As shown in the cross-sectional image in Fig. 4c, the coating is fairly uni-

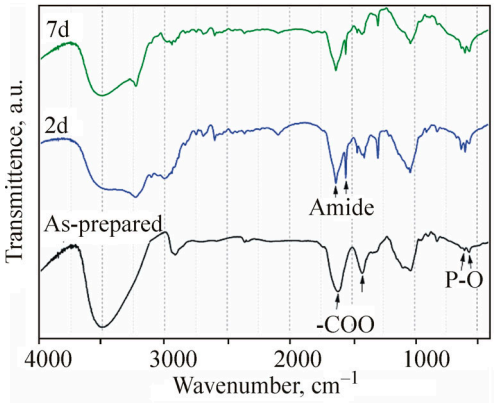

Fig. 3. FTIR spectra of the multilayer coatings before and after incubation in simulated body fluid for 2 and 7 days.

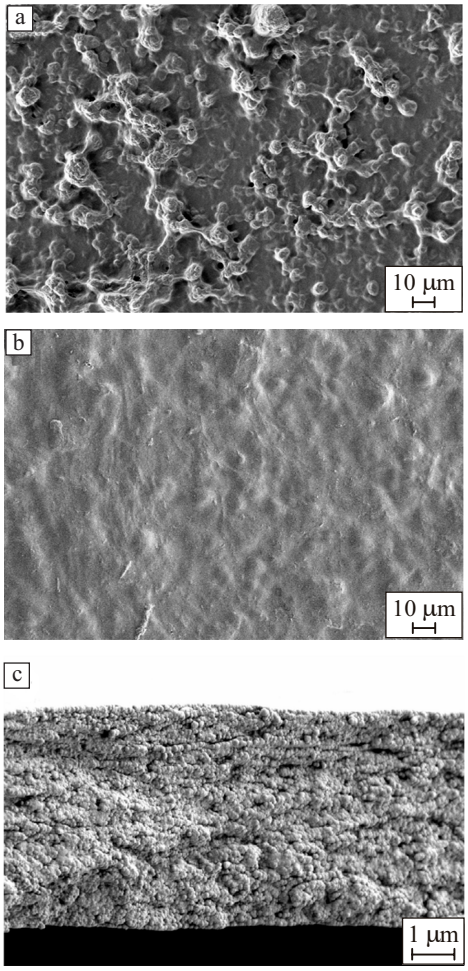

Fig. 4. SEM images of the surface of a two-EPD layer structure (a), the surface (b) and cross-section (c) of the final multilayer coating.

form in thickness (~6 μm averaged from 6 different positions in the figure) and appears rather homogeneous even after 10 separate deposition cycles, indicating the reproducibility of the final multilayer structure. In the image of the coating cross section, the layered structure is not clearly identified, which can be attributed to the good bonding between the deposited layers.

Table 2. Roughness values (Ra) of the deposited coating with/without lysozyme addition.

Coating structure	With lysozyme, μm	Without lysozyme, μm
Bottom layer	1.35 ± 0.10	1.03 ± 0.01
Two-EPD layer	0.99 ± 0.01	1.05 ± 0.04
Final multilayer	0.71 ± 0.04	0.78 ± 0.03

Surface SEM images of the deposited coating after simulated body fluid incubation for 14 days are shown in Fig. 5. The surface appears to get rougher after simulated body fluid incubation due to the initial degradation of the superficial polymer layer. Figure 5b shows a high magnification image of an open crack in Fig. 5a as highlighted in the figure. A typical mineralized apatite structure with very small crystallites is observed, which is in agreement with the morphology of hydroxyapatite coatings after simulated body fluid incubation, as reported in the literature [31]. This evidence of hydroxyapatite formation proves qualitatively the bioactivity of the deposited coating.

3.5. Surface roughness

It is suggested that the addition of polymer layers, either by electrophoretic deposition or by layer-by-layer deposition, will modify the surface roughness of the coating, therefore the surface roughness after each coating step was quantitative evaluated by laser profilometer measurements, as shown in Table 2. The arithmetic mean values of roughness (Ra) of the deposited coating, with or without lysozyme addition, decreased gradually with the number of deposited layers, which is in agreement with the SEM observation in Fig. 4. The roughness of the bottom layer, due to the addition of polymer-like lysozyme, was significantly decreased compared with the roughness of the lysozyme-free bottom layer. After the LbL deposition with the same processing parameters, the EPD layers were completely covered leading to similar surface roughness of the final multilayer coatings.

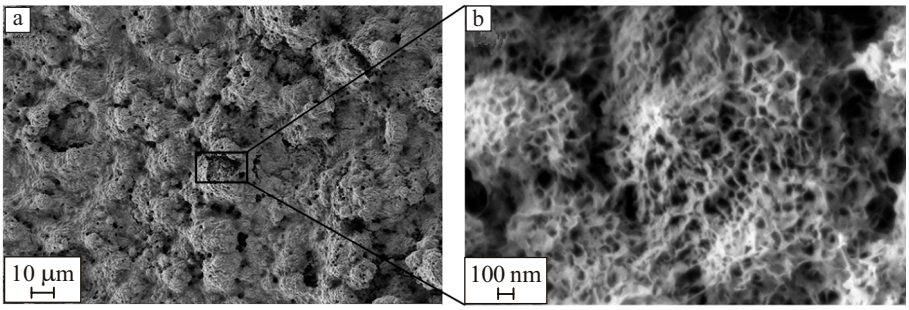

Fig. 5. Surface SEM image of the deposited coating after incubation in simulated body fluid for 14 days (a), high magnification image of the selected area (b).

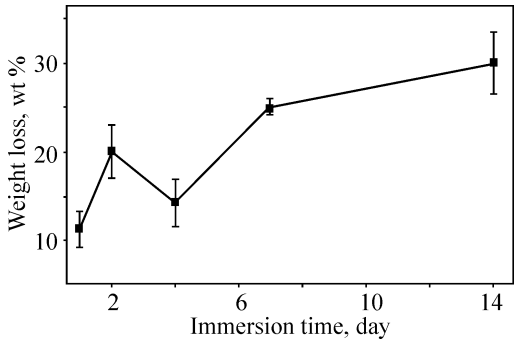

Fig. 6. Weight loss of the deposited multilayer coating (without lysozyme addition) after incubation in PBS for different time periods.

3.6. Degradation test

The degradation rate is one of the most important characteristics for a coating system especially if it should be capable of a constant and controlled drug release. Figure 6 shows the weight loss of deposited coatings, without the addition of lysozyme, as a function of immersion time in simulated body fluid for 1, 2, 4, 7, and 14 days. The deposited coating showed a ~10 wt % weight loss after 1 day of incubation. The weight loss increased to 30 wt % up to 14 days of incubation. Therefore, a potential burst release, which could occur due to the swelling and excessive dissociation of the coating structure, could be minimized in order to achieve a sustained (long-term) drug release.

3.7. Lysozyme release test

In this study, we exploited the possibility of incorporating lysozyme in the first two EPD layers as schematically shown in Fig. 1. The percentage of cumulative lysozyme release from the multilayer coating was normalized and plotted in Fig. 7. The release profiles from a two-EPD coating as well as from the multilayer coatings with different number of LbL layers were measured for comparison. Significant differences were observed as a result of the number of LbL layers. During the first 30 min, the initial release of lysozyme from the two-EPD coating was nearly 83 %, while the extent of release was significantly reduced to 45 and 12 % for the multilayer coatings with 2 and 8 LbL depositions, respectively. Subsequently, the lysozyme release was found to occur in a controlled manner over a period of 168 h (7 days) and 336 h (14 days) for these two coating structures, which is more desirable than that of the two-EPD coating showing a 97 % release over a short period of 96 h. The overall release of drugs is commonly divided into two stages: the burst release (drug released from the proximal surface or weak-connected points of the coatings) and the sustained release (drug released from the interior or strong-connected points of the coatings) [32]. It can be concluded from our experimental results that the inhibition of the initial burst release by the layered structure of the coating leads to a sustained release. Additionally, it is found that the degradation rate of the coating, which is highly associated with swelling of the coating, desorption and diffusion of biomolecules from the coating matrix, plays an important role on the release behavior. Therefore, future investigations will consider the improvement of degradation properties, especially tailoring the degradation of the different biopolymer layers, to achieve a longer drug release period.

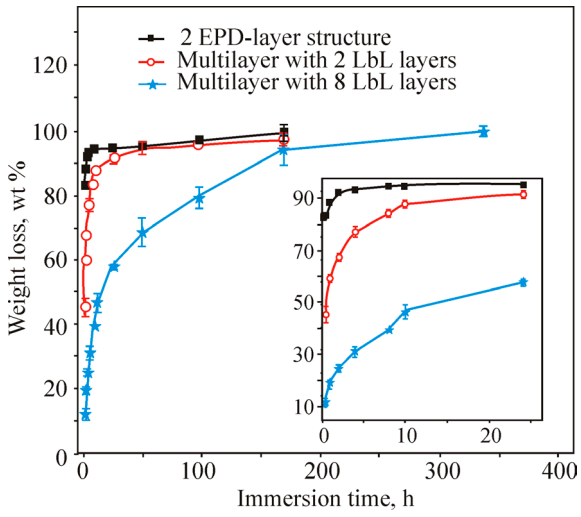

Fig. 7. Lysozyme release profile of the deposited coatings in PBS with different coating structures, the inset shows the release profile within 24 h.

3.7. Cell viability test

Cell viability of the multilayer coatings, fabricated from EPD suspensions with different concentration of lysozyme, was analyzed using the CCK8 assay (Fig. 8). The pure stainless steel substrate was selected as the control. It is found that the cell viability in lysozyme-containing coatings was lower than the control ($P < 0.001$) after 1 day of incubation, which may be due to the burst release of lysozyme

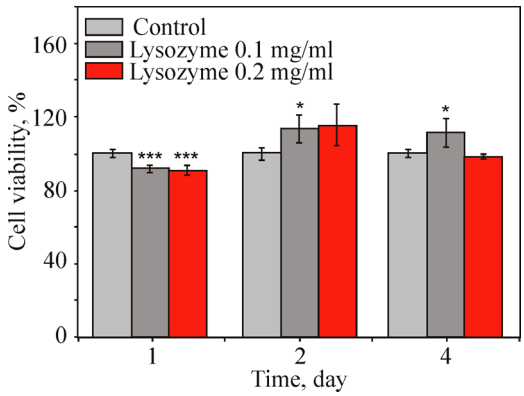

Fig. 8. Cell viability of the deposited multilayer coatings with different lysozyme concentration.

during the first day. However, the cell viability for each group remains over 90 %. After 2 days of cell culture, an increase of cell viability was found in lysozyme-containing groups, especially for the lysozyme 0.1 mg/ml sample ($P < 0.05$). The increase in the cell viability can be explained by the presence of the bioactive and biocompatible components in the bottom layer. It was noted that similar results were also found on day 4. Experimental results suggest that there is no obvious toxicity of lysozyme on MG-63 cells.

3.8. Antibacterial test

In this study, two model bacteria, *Bacillus subtilis* and *E. coli* from gram-positive and gram-negative bacteria families, respectively, were selected to evaluate the antibacterial effect of the lysozyme-containing multilayer coatings. Firstly the minimal inhibitory concentration of lysozyme against both bacteria was carried out to quantitatively validate the inhibitory efficiency of lysozyme used. A sterilized PBS solution was selected as the reference. As shown in Fig. 9, it is clearly observed that the minimal inhibitory concentration of lysozyme against *Bacillus subtilis* is 0.625 μg/ml. However the minimal inhibitory concentration study of lysozyme for *E. coli* shows little effectiveness, which is in accordance with reported results in the literature [33].

The quantitative antibacterial test was employed to evaluate the inhibitory efficiency of lysozyme-loaded coatings in the early stage of implantation. In order to evaluate whether the sustained release of lysozyme from the multilayer coating can exert an antibacterial effect after the initial burst release, firstly the lysozyme-loaded multilayer coatings were immersed in PBS in a 37 °C incubator for 1, 3 and 7 days. After each time point the solutions were replaced with 2 ml of fresh PBS and incubated for other 12 h. The lateral extracted solutions were subjected to antibacterial test. As shown in Fig. 10, the extracted solution can effectively inhibit the growth of *Bacillus subtilis* as the maximum bacterial growth of day 7 sample is only 6 %, in other words the minimum inhibitory efficiency is as high as 94 %. The excellent antibacterial effect against gram-positive bacteria is attributed to the lysozyme concentration which is higher than minimal inhibitory concentration.

The antibacterial test indicated that the proposed multilayer coating could be useful for loading and releasing lysozyme in a controlled manner leading to antibacterial effect. Lysozyme is a well-known lytic enzyme found in many natural systems, however its limited antibacterial efficacy against gram-negative bacteria restricts its application in the biomedical field. Many investigations have been carried out on the extension of the antimicrobial spectrum of lysozyme to gram-negative bacteria including denaturation of lysozyme, attachment of other compounds to lysozyme molecular structure, and the use of membrane permeabilizing agents with lysozyme, for example EDTA [34, 35]. Apart from those strategies, in the case of our multilayer structure, it is possible that additional antibacterial agents, e.g. biomolecules or nanoparticles, which are specific for the inhibition of gram-negative bacteria, could be incorporated into the coating structure to achieve a simultaneous dual release. In this context, previous work has confirmed that gold or silver nanoparticles could be effectively combined with lysozyme for enhanced antibacterial purposes in coating structures [36, 37].

4. Conclusions

Multilayered bioactive coatings, constituted by hydroxyapatite and antibacterial lysozyme embedded in biopolymer coatings, have been successfully fabricated by a combination of electrophoretic deposition and layer-by-layer deposition. Increased deposit yield and reduced surface roughness of the deposited coating as a function of the number of layers were observed. More importantly, stable deg-

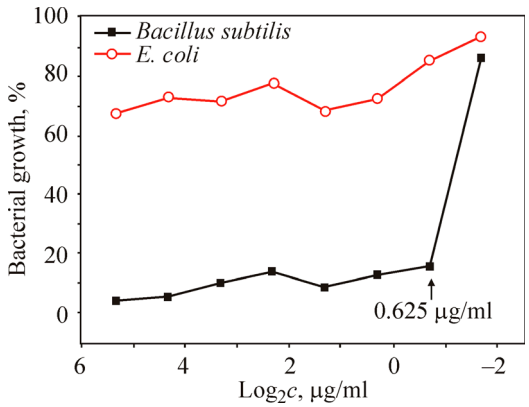

Fig. 9. Minimal inhibitory concentration tests of lysozyme against gram-positive *Bacillus subtilis* and gram-negative *E. coli*. Lysozyme was dissolved in sterilized PBS solution and the dilution starts from 40 μg/ml.

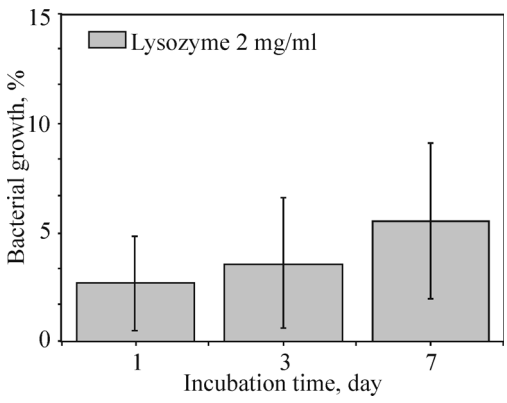

Fig. 10. Quantitative antibacterial effect of the deposited multilayer coating after incubation in PBS for 1, 3, and 7 days against *Bacillus subtilis*. The concentration of the extracted lysozyme solution for 1, 3 and 7 days are 31.7, 12.3, 3.0 μg/ml, respectively.

radation rate of the multilayer coating was achieved and the initial burst release of the biomolecule was suppressed obtaining a sustained release of lysozyme up to 14 days. No obvious cytotoxic effect of lysozyme on MG-63 cells was found according to CCK-8 assay. Quantitative antibacterial tests indicated that lysozyme released from the multilayer coating incubated in PBS for 7 days was still effective to inhibit the growth of gram-positive bacteria (94 % of inhibition). Suggestions for future work include the improvement of the degradation rate and the incorporation of additional antibacterial agents for an extended antimicrobial spectrum for drug delivery purposes for applications in orthopedic implants.

Acknowledgements

We thank Ms. S. Link and Mr. L. Cordero-Arias (Institute of Biomaterials, University of Erlangen-Nuremberg, Germany) for experimental support. Qiang Chen (No. 2011629002), Yufang Liu (No. 201206790009) and Kai Zheng (No. 201206740003) gratefully acknowledge the China Scholarship Council (CSC) for financial support. The authors acknowledge the support from Chinese National Nature Science Foundation (No. 21374081).

Reference

1. Salinas AJ, Vallet-Regi M. Bioactive ceramics: from bone grafts to tissue engineering. RSC Adv. 2013; 3: 11116–11131.
2. Goodman SB, Yao Z, Keeney M, Yang F. The future of biologic coatings for orthopaedic implants. Biomaterials. 2013; 34: 3174–3183.
3. Shah NJ, Hong J, Hyder MN, Hammond PT. Osteophilic multilayer coatings for accelerated bone tissue growth. Adv Mater. 2012; 24: 1445–1450.
4. Whitehouse JD, Friedman ND, Kirkland KB, Richardson WJ, Sexton DJ. The impact of surgical-site infections following orthopedic surgery at a community hospital and a university hospital: adverse quality of life, excess length of stay, and extra cost. Infect Control Hosp Epidemiol. 2002; 23: 183–189.
5. Campoccia D, Montanaro L, Arciola CR. The significance of infection related to orthopedic devices and issues of antibiotic resistance. Biomaterials. 2006; 27: 2331–2339.
6. Lazzarini L, Lipsky B, Mader JT. Antibiotic treatment of osteomyelitis: what have we learned from 30 years of clinical trials? Int J Infect Dis. 2005; 9: 127–138.
7. Pishbin F, Mouriño V, Gilchrist JB, McComb DW, Kreppel S, Salih V, Ryan MP, Boccaccini AR. Single-step electrochemical deposition of antimicrobial orthopaedic coatings based on a bioactive glass/chitosan/nano-silver composite system. Acta Biomater. 2013; 9: 7469–7479.
8. Donlan R. Biofilms: Microbial life on surfaces. Emerg Infect Dis. 2002; 8: 881–890.
9. Besra L, Liu M. A review on fundamentals and applications of electrophoretic deposition (EPD). Prog Mater Sci. 2007; 52: 1–61.
10. Corni I, Ryan MP, Boccaccini AR. Electrophoretic deposition: From traditional ceramics to nanotechnology. J Eur Ceram Soc. 2008; 28: 1353–1367.
11. Boccaccini AR, Keim S, Ma R, Li Y, Zhitomirsky I. Electrophoretic deposition of biomaterials. J R Soc Interface. 2010; 7: S581–S613.
12. Seuss S, Boccaccini AR. Electrophoretic deposition of biological macromolecules, drugs, and cells. Biomacromolecules. 2013; 14: 3355–3369.
13. Zhitomirsky D, Roether JA, Boccaccini AR, Zhitomirsky I. Electrophoretic deposition of bioactive glass/polymer composite coatings with and without HA nanoparticle inclusions for biomedical applications. J Mater Process Technol. 2009; 209: 1853–1860.
14. Chen Q, Cabanas-Polo S, Goudouri OM, Zhitomirsky I. Electrophoretic co-deposition of polyvinyl alcohol (PVA) reinforced alginate–Bioglass® composite coating on stainless steel: Mechanical properties and in-vitro bioactivity assessment. Mater Sci Eng C. 2014; 40: 55–64.
15. Dorozhkin SV. Bioceramics of calcium orthophosphates. Biomaterials. 2010; 31: 1465–1485.
16. Giannoudis PV, Dinopoulos H, Tsiridis S. Bone substitutes: An update. Injury. 2005; 26: S20–S27.
17. Lee KY, Mooney DJ. Alginate: Properties and biomedical applications. Prog Polym Sci. 2012; 37: 106–126.
18. Nair LS, Laurencin CT. Biodegradable polymers as biomaterials. Prog Polym Sci. 2007; 32: 762–798.
19. Ordikhani F, Tamjid E, Simchi A. Characterization and antibacterial performance of electrodeposited chitosan–vancomycin composite coatings for prevention of implant-associated infections. Mater Sci Eng C. 2014; 41: 240–248.
20. Chuang HF, Smith RC, Hammond PT. Polyelectrolyte multilayers for tunable release of antibiotics. Biomacromolecules. 2008; 9: 1660–1668.
21. Burke SE, Barrett CJ. pH-dependent loading and release behavior of small hydrophilic molecules in weak polyelectrolyte multilayer films. Macromolecules. 2004; 37: 5375–5384.
22. Zimmerli W, Trampuz A, Ochsner PE. Prosthetic-joint infections. N Engl J Med. 2004; 351: 1645–1654.
23. Borges J, Mano JF. Molecular interactions driving the layer-by-layer assembly of multilayers. Chem Rev. 2014; 114: 8883–8942.
24. Caridade SG, Monge C, Gilde F, Boudou T, Mano João, Picart C. Free-standing polyelectrolyte membranes made of chitosan and alginate. Biomacromolecules. 2013; 14: 1653–1660.
25. Kokubo T, Takadama H. How useful is SBF in predicting *in vivo* bone bioactivity? Biomaterials. 2006; 27: 2907–2915.
26. Pritchard SR, Phillips M, Kailasapathy K. Identification of bioactive peptides in commercial cheddar cheese. Food Res Int. 2010; 43: 1545–1548.
27. Hamaker HC. Formation of a deposit by electrophoresis. Trans Farad Soc. 1940; 36: 279–283.
28. Chen Q, Coedero-Arias L, Roether JA, Cabanas-Polo S, Virtanen S, Boccaccini AR. Alginate/Bioglass® composite coatings on stainless steel deposited by direct current and alternating current electrophoretic deposition. Surf Coat Technol. 2013; 233: 49–56.
29. Jao WC, Chen HC, Lin CH, Yang MC. The controlled release behavior and pH- and thermo-sensitivity of alginate/poly(vinyl alcohol) blended hydrogels. Polym Adv Technol. 2009; 20: 680–688.
30. Lawrie G, Keen I, Drew B, Chandler-Temple A, Rintoul L, Fredericks P, Grondahl L. Interactions between alginate and

chitosan biopolymers characterized using FTIR and XPS. Biomacromolecules. 2007; 8: 2533–2541.
31. Zheng X, Huang M, Ding C. Bond strength of plasma-sprayed hydroxyapatite/Ti composite coatings. Biomaterials. 2000; 21: 841–849.
32. Kong Z, Yu M, Cheng K, Weng W, Wang H, Lin J, Du P, Han G. Incorporation of chitosan nanospheres into thin mineralized collagen coatings for improving the antibacterial effect. Colloids Surf B. 2013; 111: 536–541.
33. Hughey VL, Wilger PA, Johnson EA. Antibacterial activity of hen egg white lysozyme against Listeria monocytogenes Scott A in foods. Appl Environ Microbiol. 1989; 55: 631–638.
34. Park SL, Daeschel MA, Zhao Y. Antimicrobial chitosan-lysozyme (CL) films and coatings for enhancing microbial safety of mozzarella cheese. J Food Sci. 2006; 69: M215–M221.
35. Padgett T, Han IY, Dawson PL. Incorporation of food-grade antimicrobial compounds into biodegradable packaging films. J Food Prot. 1998; 61: 1330–1335.
36. Su Y, Li C. Stable multilayer thin films composed of gold nanoparticles and lysozyme. Appl Surf Sci. 2008; 254: 2003–2008.
37. Eby DM, Luckarift HR, Johnson GR. Hybrid antimicrobial enzyme and silver nanoparticle coatings for medical instruments. Appl Mater Interfaces. 2009; 1: 1553–1560.